

## Optical Properties of Poly (Vinyl Chloride-co-Vinyl Acetate-co-2-Hydroxypropyl Acrylate) / (Acrylonitrile-Butadiene-Styrene) Blends

T. Fahmy<sup>1,2\*</sup>, A. Sarhan<sup>2</sup>, I. A. Elsayed<sup>1,3</sup> H. G. Abelwahed<sup>1,4</sup>

<sup>1)</sup>Plasma Technology and Maaterial Science Unit (PTMSU), Physics Department, College of Science and Humanity, Prince Sattam bin Abdulaziz University, KSA.

<sup>2)</sup> Polymer Resrech Group, Physics Department, Faculty of Science, Mansoura University, 35516 Mansoura, EGYPT.

<sup>3)</sup>Physics Department, Faculty of Science, Damitta University, Damitta, EGYPT.

<sup>4)</sup>Theoretical Physics Group, Physics Department, Faculty of Science, Mansoura University, 35516 Mansoura, EGYPT.

### ABSTRACT

The morphology and optical properties of PVVH, ABS and its polyblend samples have been studied using different techniques such as atomic force microscopy, AFM, Fourier transform-Infrared, FTIR, Raman spectroscopy and UV-Vis spectroscopy. AFM images showed that roughness of polyblend samples is increased as PVVH content is decreased in the polyblend samples. FTIR spectroscopy has been investigated for PVVH, ABS and its polyblend samples in the range from 4000 to 500  $\text{cm}^{-1}$ . The characteristic absorption bands of PVVH and ABS are detected. On the other hand, the main absorption bands of pure materilas have been affected in their positions and intensities in the FTIR spectra of polyblend samples. Raman Spectroscopy is carrid out for all the samples in the range 3650-50  $\text{cm}^{-1}$ . Analysis of UV spectroscopy showed that absorption edge and indirect optical energy gap are decreased with decreasing PVVH content in polyblend samples.

**Keywords:** PVVH, ABS, Polyblend, Miscibility, AFM, Raman shift.

### INTRODUCTION

The polymer blends have been attracted much attention in the area of research and development in polymer science in the past three decades, because of their

potential usage in many applications, such as, electro-optical devices, pipes, sensor technology, shielding, polymer electrolytes and membranes [1-6]. One of the commercial advantages is that polymer blends provide a method to produce new materials with new property profiles, which reduces development costs. Polymer blending is an interesting method for investigating the phase separation and polymer interactions at microscopic and mesoscopic levels.

ABS terpolymer is widely used in engineering thermoplastics containing rubber. It is characterized by two phase systems with a glassy poly (styrene acrylonitrile), (SAN) copolymer and a rubbery polybutadiene (PB). PVVH is an amorphous terpolymer and has a sensitive chemical structure to variation of temperature. The properties of polymer blends can be improved by varying composition ratio and conditions of the processing. Both dipole-dipole interaction and hydrogen bonding are responsible for polymer-polymer compatibility and miscibility [7-8].

The investigation of both optical properties and electrical properties of polyblend materials is very important as well as the study of their thermal and mechanical properties. The present article is devoted for investigating the morphology and optical properties of PVVH/ABS polymer blend.

## **Experimental Work**

Poly (vinyl chloride-co-vinyl acetate-co-2-hydroxypropyl acrylate), PVVH, is supplied from Aldrich Chemicals. Acrylonitrile-butadiene-styrene, ABS, is supplied from Poly Sci., USA. The films of samples are prepared using casting method. Tetrahydrofuran (THF) is used a common solvent for PVVH and ABS. The solvent was eliminated in an oven, at temperature of  $\sim 323$  K for two days.

Atomic force microscope (AFM) is investigated using Bruker Dimension Icon system with Scan Asys mode (tapping). Fourier- Transform Infrared Spectroscopy, FT-IR, is carried out in the range from 4000 to 500  $\text{cm}^{-1}$  using FT-IR spectroscopy, Omnic. Raman Spectroscopy is carried out using Senterra II, Bruker in the range 3650-50  $\text{cm}^{-1}$ . Ultra violet-Visible (UV-Vis) spectroscopy is carried out in the range from 200 to 800 nm by UV 5200 Spectrophotometer, at Physics Department, College of Science and Humanities, Prince Sattam bin Abdulaziz University.

## **RESULTS and DISCUSSION**

### **Atomic Force Microscope (AFM)**

The AFM amplitude and three-dimensional (3D) height images of PVVH, ABS and its polyblend samples are shown in Fig. 1. Large numbers of hills and valleys are observed in the 3D height images. AFM images in Fig. 1 exhibited surface with some agglomerates and low amplitude of roughness.

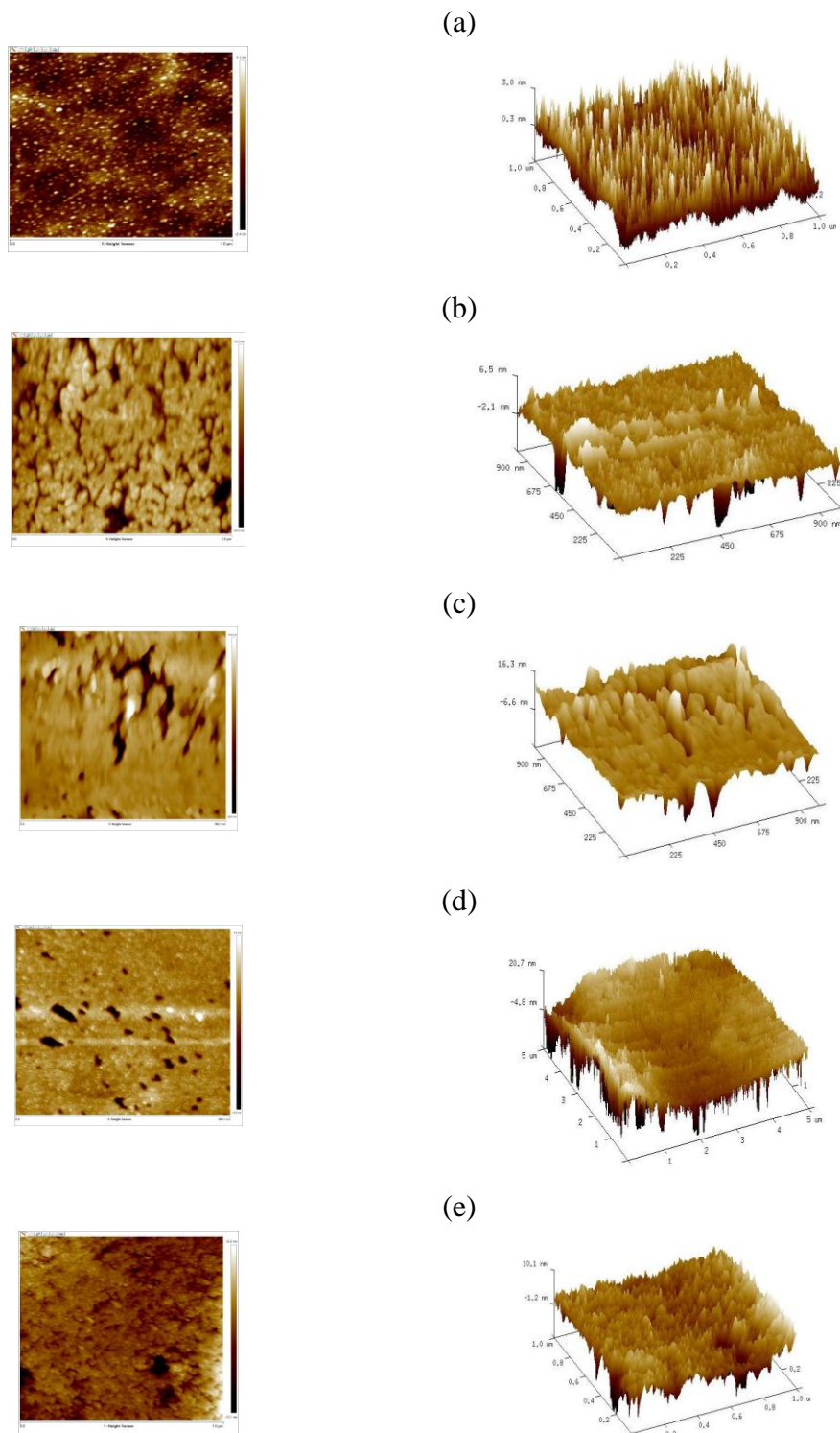


**Figure 1:** AFM images of a) PVVH, b) 70wt% PVVH, c) 50 wt% PVVH, d) 30 wt% PVVH and e) ABS.

The values of  $R_{ms}$ ,  $R_a$  and surface area of the samples are estimated and summarized in Table 1. Generally, the values of both  $R_{ms}$  and  $R_a$  will be similar to each other if the sample surface is flat and does not contain any deviations from the mean surface level. On the other hand, values of  $R_{ms}$  will be greater than  $R_a$  if the surface of the sample is very rough and contains significant numbers of holes and large bumps [9]. From the  $R_{ms}$  and  $R_a$  values of these blends in Table 1, one can conclude that the surfaces of the polyblend samples are very rough and large bumps and holes are found in appreciable numbers.

**Table 1:** The values of  $R_a$ ,  $R_q$ ,  $R_{max}$  and surface area of all samples.

Material	Average surface roughness $R_a$ (nm)	RMS surface roughness $R_q$ (nm)	Average height $R_{max}$ (nm)	Surface area ( $\mu\text{m}^2$ )
PVVH	0.57	0.74	12.1	1.04
70 wt% PVVH/ 30 wt% ABS	0.92	1.90	34.5	26.3
50 wt% PVVH/ 50 wt% ABS	2.97	4.99	49.1	1.07
30 wt% PVVH/ 70 wt% ABS	4.41	6.23	83.3	1.03
ABS	1.75	2.53	30.7	1.06

### Fourier Transform- Infrared (FTIR)

FTIR spectroscopy is a highly effective method to examine the polymer-polymer interactions. This method is used extensively to investigate the mechanism of interpolymer miscibility qualitatively and quantitatively through the hydrogen bonding [10-12]. FTIR spectrum of pure PVVH is characterized by bands at 2968 and 2916  $\text{cm}^{-1}$  are related to *C-H stretches*, 1733  $\text{cm}^{-1}$  is attributed to *C=O*, 1441  $\text{cm}^{-1}$  is attributed to *CH<sub>3</sub> rocking*, 1385, 1329, 1251, 1094, and 1049  $\text{cm}^{-1}$  are attributed to *C-O stretch coupled with C-C vibration*, 966  $\text{cm}^{-1}$  is attributed to skeletal vibrations and 691 and 615  $\text{cm}^{-1}$  are attributed to *C-Cl stretches and skeletal vibrations*, as shown in Fig. 2a [13-15]. FTIR spectrum of ABS is characterized by many absorption peaks, such as, 2234  $\text{cm}^{-1}$  and 1452  $\text{cm}^{-1}$ , as shown in Fig. 2e. These bands are attributed to nitrile group in ABS, i.e.,  $\text{C}\equiv\text{N}$  and double bonds of butadiene blocks. The absorption at 1677 and 1495  $\text{cm}^{-1}$  are related to styrene double bonds in ABS terpolymer. The absorption band at 2851  $\text{cm}^{-1}$  is attributed to the vibration of aliphatic and aromatic C-H bond. Also, the bands at 3022  $\text{cm}^{-1}$  and 2926  $\text{cm}^{-1}$  are related to aromatic C-H bonds and the vibration of aliphatic [16]. The bands at 700 and 755  $\text{cm}^{-1}$  are related to C-H *def* (out of phase) and at 964  $\text{cm}^{-1}$  is related to  $\text{C}=\text{C}-\text{H}$  *def* (aliphatic). On the other hand, it is observed that FTIR spectra of PVVH/ABS polyblend samples exhibit all the characteristic absorption spectral bands of PVVH and ABS with some changes in both their intensities and positions, such as 2234  $\text{cm}^{-1}$ , 1670  $\text{cm}^{-1}$  and 1452  $\text{cm}^{-1}$ ,

as displayed in Fig. 2(b-d). This behavior is confirming to the high miscibility of the polyblend due to the formation of hydrogen bonding between the functional groups of both polymers [6].

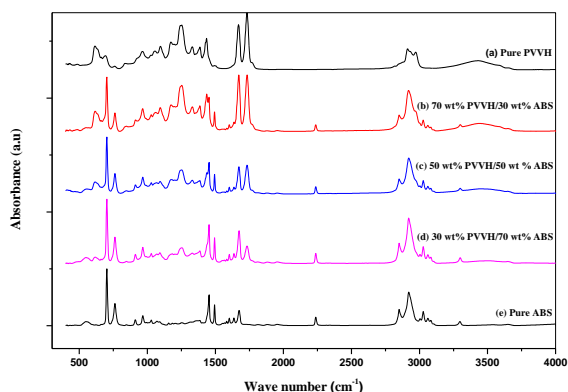


**Figure 2:** FTIR spectrum of PVVH, ABS and samples of polyblends.

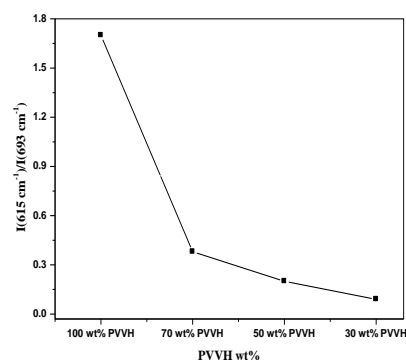


**Figure 3:** Ratio of  $I(615\text{ cm}^{-1})/I(692\text{ cm}^{-1})$  versus PVVH wt %.

The intensity ratio of both  $638\text{ cm}^{-1}$  and  $692\text{ cm}^{-1}$  absorption peaks [ $I(638\text{ cm}^{-1})/I(691\text{ cm}^{-1})$ ] is highly sensitive for any change in the molecular conformation and structure of the crystal [17]. It is observed that, this ratio of PVVH/ABS polyblend samples is decreased as PVVH content decreased, as shown in Fig. 3. Also, it is observed the intensity of many absorption bands such as  $1733\text{ cm}^{-1}$ ,  $1251\text{ cm}^{-1}$  and  $966\text{ cm}^{-1}$  has been decreased as the content of PVVH is decreased in the polyblend samples, as shown in Fig. 4.

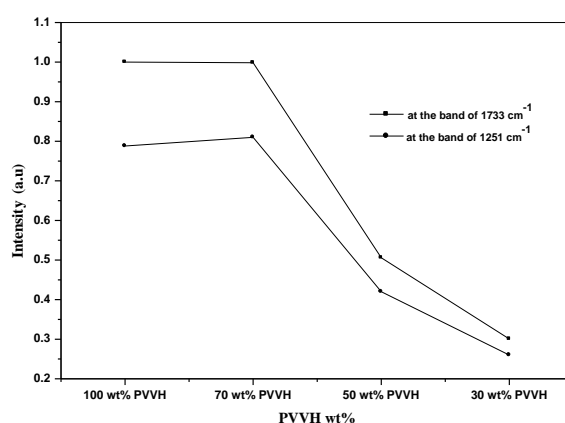


**Figure 4:** The intensity of the bands  $1733\text{ cm}^{-1}$  and  $1251\text{ cm}^{-1}$  versus PVVH content.

## Raman Spectroscopy

The advantage of Raman spectroscopy technique is its high sensitivity to nonpolar bonds and its ability to give qualitative and quantitative information on the macromolecules in various configurational and phase states, involving the description of different crystalline modifications and amorphous regions having different states of order [18]. Fig. 5a displays Raman spectrum of pure PVVH. It is observed that, Raman spectrum of PVVH is characterized by seven obvious bands located at  $639\text{ cm}^{-1}$ ,  $695\text{ cm}^{-1}$ ,  $860\text{ cm}^{-1}$ ,  $1105\text{ cm}^{-1}$ ,  $1381\text{ cm}^{-1}$ ,  $1870\text{ cm}^{-1}$ ,  $2920\text{ cm}^{-1}$  and  $3283\text{ cm}^{-1}$ , respectively. The band at  $2920\text{ cm}^{-1}$  is attributed to C-H stretching. The band at  $1381\text{ cm}^{-1}$  is related to the twist or bending of  $\text{CH}_2$  and  $\text{CH}_3$  bonds. The region of  $1000\text{--}1150\text{ cm}^{-1}$  involves C-C stretching vibrations and this region is very sensitive to the conformational changes, i.e., the properties of the bands in this region has been modified, as shown in Fig. 5c for the PVVH/ABS polyblend samples [17]. The bands in the region  $639\text{--}690\text{ cm}^{-1}$  are related to the C-Cl stretching. Raman spectrum of ABS is characterized by three bands detected at  $1604\text{ cm}^{-1}$ ,  $1666\text{ cm}^{-1}$  and  $2238\text{ cm}^{-1}$ , as shown in Fig. 5b. These bands are attributed to styrene, butadiene and acrylonitrile phases, respectively.

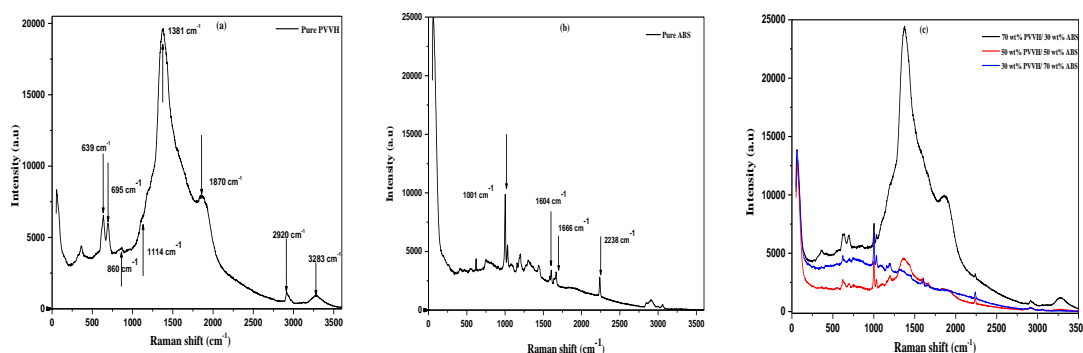


**Figure 5:** Raman shift of a) PVVH, b) ABS and c) polyblend amples.

## UV-Vis Spectroscopy

The electronic structure of polymeric materials can be studied by investigation its optical absorption. The absorption is occurred when the photon has an enough amount of energy to excite the electrons from lowest energy to highest energy levels. Based on Davis–Mott model, the wave function is localized and the transition probability depends mainly on the overlapping of wave functions [19]. In the amorphous material, the localized states extend from the conduction and valence bands to the energy gap band. Hence, these localized states can affect the electron transition in polymeric materials [20].

UV spectra of PVVH, ABS and its polyblends have been investigated in the range of wavelength from 200 to 850 nm, as shown in Fig. 6a. The investigation of optical

absorption gives more valuable information regarding the band structure of polymeric materials. The absorption coefficient of all samples is calculated using the following equation [21]

$$\alpha(\nu) = 2.303 \frac{A}{d}$$

Where,  $A$  and  $d$  are defined as the absorbance and thickness of the sample, respectively. The valuable information of both the optical energy band gap ( $E_g$ ) and electronic band structure can be obtained using absorption coefficient ( $\alpha$ ). Fig. 6b displays the variation of optical absorption coefficient ( $\alpha$ ) against photon energy ( $h\nu$ ) for all samples. The values of absorption edge are calculated by extrapolating the linear portion of  $\alpha$  to zero absorption value and summarized in Table 1. On the other hand, the optical energy band gap ( $E_g$ ) values for pure and polyblend samples are calculated using the following formula [22]

$$\alpha = B \frac{(h\nu - E_g)^n}{h\nu}$$

Where,  $B$  is a constant and depends mainly on probability of the transition and localized state width inside the band gap,  $h\nu$  is the photon energy,  $n$  is an index depends on the transition nature and is attributed to the density of states distribution. For the allowed direct and indirect transitions,  $n$  will equal to 1/2 and 2, whereas, for forbidden direct and indirect transition  $n$  equals to 3/2 and 3, respectively. Fig. 6c shows  $(\alpha h\nu)^2$  against  $h\nu$  for all samples under investigation. The allowed indirect optical energy gap values are estimated from the intercept of the extrapolated linear portion of  $(\alpha h\nu)^2$  on the photon energy axis, as shown in Fig. 6c, and summarized in Table 1.

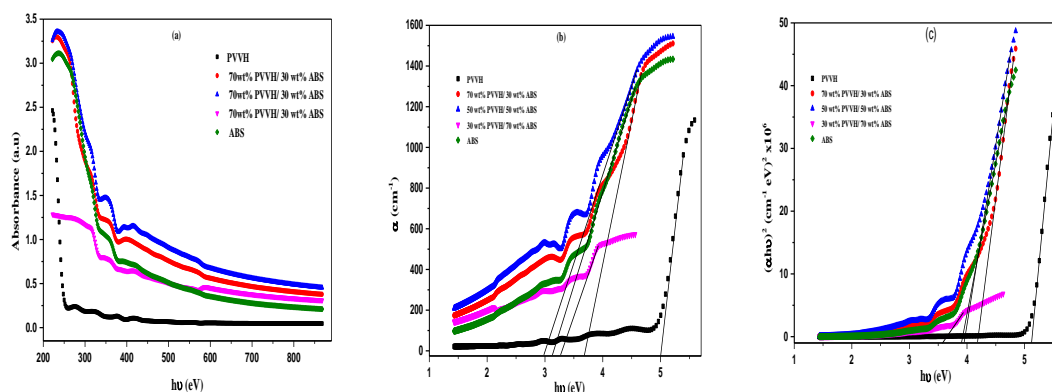


**Figure 6:** a) Absorbance, b) Absorbance coefficient ( $\alpha$ ) and c)  $(\alpha h\nu)^2$  versus  $h\nu$  for pure and polyblend samples.

It is observed that with decreasing PVVH content the optical band gap of PVVH/ABS polyblend samples are decreased. This behavior can be interpreted based on the increasing in the number of unsaturated defects will increase the final

states density in the band structure resulting in low optical band gap energy or may attributed to structural rearrangement [23].

The physical processes that primarily control the behavior of the gap states in the amorphous polymeric materials are structural disorder which responsible for structural defects and tail states in deep states. The lattice configuration fluctuation in polymeric materials will distort the fundamental edge resulting in Urbach tail [22]. Fig. 7 displays the variation of  $\ln \alpha$  against  $h\nu$  for all samples to get some information about the band tails. The values of Urbach energy ( $E_U$ ) are calculated using the slope of linear relationship of  $(\ln \alpha)$  versus  $(h\nu)$  using the following equation

$$\alpha(\nu) = \alpha_0 \exp\left(\frac{h\nu}{E_U}\right)$$

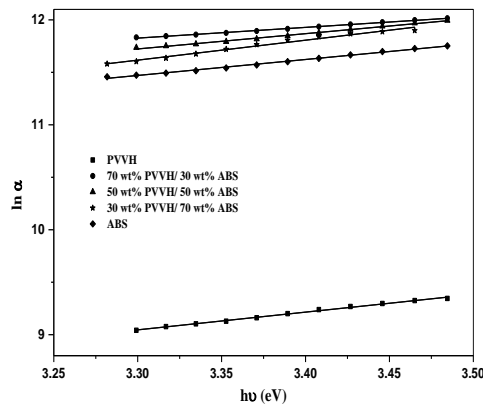


**Figure 7:**  $\ln \alpha$  against photon energy  $h\nu$ .

where  $\alpha_0$  and  $E_U$  are defined as a constant and Urbach energy, respectively and is often explained as the tail of localized states width in the band gap. The exponential tail is appeared because amorphous and/or disordered materials produce extended localized states in the bandgap.

**Table 1:** The values of Absorption Edge, Optical Energy Gap and Urbach energy of all samples.

Material	Absorption Edge (eV)	Optical Energy Gap (eV)	Urbach enegy (eV)
PVVH	4.88	5.12	0.60
70 wt% PVVH/ 30 wt% ABS	3.68	4.17	0.98
50 wt% PVVH/ 50 wt% ABS	2.97	3.94	0.69
30 wt% PVVH/ 70 wt% ABS	3.27	3.59	0.53
ABS	3.12	3.91	0.66



## CONCLUSION

AFM images of pure and polyblend samples revealed that the roughness of sample surface is increased as PVVH content is decreased in the polyblend samples. FTIR spectroscopy has been investigated for PVVH, ABS and its polyblend samples. It is found that FTIR of PVVH is characterized by main absorption bands at  $2968\text{ cm}^{-1}$ ,  $1733\text{ cm}^{-1}$ ,  $1441\text{ cm}^{-1}$ ,  $691\text{ cm}^{-1}$  and  $615\text{ cm}^{-1}$ , while the absorption bands characterizing acrylonitrile, butadiene and styrene of ABS are obtained at  $2234\text{ cm}^{-1}$ ,  $1452\text{ cm}^{-1}$ ,  $1677\text{ cm}^{-1}$  and  $1495\text{ cm}^{-1}$ . On the other hand, the main absorption bands of pure materials have been affected in their positions and intensities due to the blending, as observed in both FTIR and Raman spectra, confirming the high miscibility between the polymers. Analysis of UV spectroscopy showed that absorption edge, indirect optical energy gap and Urbach energy are decreased with decreasing PVVH content in polyblend samples. This behavior is attributed to structural rearrangement.

## ACKNOWLEDGEMENT

We would like to thank Prince Sattam bin Abdulaziz University and Scientific Research Deanship for their supporting. This work is supported by Scientific Research Deanship in Prince Sattam bin Abdulaziz University, Saudi Arabia under Grant No.2015/01/4353.

## REFERENCES

- [1] A. Sangroniz, A. Gonzalez, L. Martin, L. Irusta, M. Iriarte, A. Etxeberria, Miscibility and degradation of polymer blends based on biodegradable poly(butylene adipate-co-terephthalate), *Polymer Degradation and Stability*, 151 (2018) 25-35.
- [2] J. Kowalonek, Surface studies of UV-irradiated poly(vinyl chloride)/poly(methyl methacrylate) blends, *Polymer Degradation and Stability* 133 (2016) 367-377.
- [3] N. Reddeppa, A.K. Sharma, V.V.R. Narasimha Rao, W. Chen, AC conduction mechanism and battery discharge characteristics of (PVC/PEO) polyblend films complexed with potassium chloride, *Measurement* 47 (2014) 33-41.
- [4] T. Fahmy, Dielectric Relaxation Spectroscopy of Poly (Vinyl Chloride-co-Vinyl Acetate-co-2-Hydroxypropyl Acrylate) / Poly (Acrylonitrile-Butadiene-Styrene) Polymer Blend, *Polymer-Plastics Tech. & Eng.*, 46 (2007) 7-18.
- [5] T. Fahmy and M. T. Ahmed, Alpha relaxation study in Poly (vinyl chloride)/poly(ethyl methacrylate) blends using thermally stimulated currents, *Polym. Inter.*, 49 (2000) 669-677.
- [6] M. D. Migahed and T. Fahmy, Structural relaxation around the glass-transition temperature in amorphous polymer blends: temperature and composition

- dependence, *Polymer*, 35 (1994) 1688-1693.
- [7] R. A. Hermosilla, A.A. Broekhuis, F. Picchioni, Reversible polymer networks containing covalent and hydrogen bonding interactions, *Eur. Polym. J.* 50 (2014) 127–134.
- [8] M. D. Migahed, M. Ishra and T. Fahmy, Rate theory and cooperative structural relaxation in amorphous polymer blends as revealed by thermal sampling study, *J. Phys. D: Appl. Phys.*, 27 (1994) 2216-2222.
- [9] M. R. Kamal, Z. Tang, T. Huang, Morphological Characterization of PE Blown Films by Atomic Force Microscopy, *International Polymer Processing*, 16(4) (2001) 376–387.
- [10] M. R. Reddy, M. J. Reddy, A. R. Subrahmanyam, Structural, Thermal and Optical Properties of PMMA, PEO and PMMA/PEO/LiClO<sub>4</sub> Polymer Electrolyte Blends, *Material Science Research India*, 14 (2017) 123-127.
- [11] T. Fahmy, Dielectric Relaxation and Electrical Conductivity Study in Thiourea-Doped Poly (Vinyl Alcohol), *Intern. J. Polymeric Mater.*, 50 (2001) 109-127.
- [12] T. Fahmy, A. Sarhan, I. A. Elsayed, M. T. Ahmed, Effect of UV Irradiation on The Structure and Optical Properties of PVA/CuCl<sub>2</sub>, *J. of Advances in Physics*, 14(2) (2018) 5378-5387.
- [13] D. Dolphin, A. Wick, *Tabulation of Infrared Spectral Data*, Wiley, NY, (1977).
- [14] R. G. J. Miller, H. A. Willis, (Eds.), *Infrared Structural Correlation Tables and Data Cards*, Heyden & Son Ltd., Spectrum House, London, (1969).
- [15] A. Gal'ikov', J. Subrt, Z. Bastl, J. Kupík, J. Blazevska-Gilev, J. Pola, Thermal degradation of poly(vinyl chloride-co-vinyl acetate) and its laser-derived analogue, *Thermochimica Acta*, 447 (2006) 75-80.
- [16] T. Fahmy, M. T. Ahmed, Thermal induced structural change investigations in PVC/PEMA polymer blend, *Polym. Testing* 20 (2001) 477-484.
- [17] L. Zhang, Jun-He Yang, Xian-Ying Wang, X. He, B. Zhao, Zhi-Hong Tang, Guang-Zhi Yang and Han-Xun Qiu, Thermal Properties of Poly(vinyl chloride-co-vinyl acetate-co-2-hydroxypropyl acrylate) (PVVH) Polymer and Its Application in ZnO Based Nanogenerators, *Chin. Phys. Lett.*, 28(1) (2011) 016501-016503.
- [18] R. L. McCreery, *Raman Spectroscopy for Chemical Analysis*, vol. 157. John Wiley & Sons, NY, (2000).
- [19] N. F. Mott, E. A. Davis, Conduction in non-crystalline systems, *Philosophical Magazine*, 17 (1968) 1269-1284.
- [20] A. N. Alias, Z. M. Zabidi, A.M.M. Ali, M. K. Harun, M.Z.A. Yahya, Optical Characterization and Properties of Polymeric Materials for Optoelectronic

- and Photonic Applications, *Inter. J of Appl. Sci. &Tech.*, 3 (2013) 11-38.
- [21] J. Tauc, *Amorphous and Liquid Semiconductors*, Springer US, (1974).
- [22] J. Tauc, A. Menth, States in the gap, *J. Non-Cryst. Solids* 8 (1972) 569–585.
- [23] C.H. Cholakis, W. Zingg, M.V. Sefton, Effect of heparin-pva hydrogel on platelets in a chronic canine arterio-venous shunt, *J. Biomed. Mater. Res.* 23 (1989) 417–441.

